

## 13A.3 Turbulence Anisotropy in the Atmospheric Boundary Layer

Cheryl Klipp

US Army Research Laboratory, Adelphi, Maryland  
20<sup>th</sup> Boundary Layers and Turbulence, 18<sup>th</sup> Air-Sea  
9-13 July, 2012, Boston, Massachusetts

### 1. Abstract

The smallest scales of turbulence are isotropic, but the larger eddies, which contain more energy, are anisotropic. The scales of maximum turbulent kinetic energy (TKE) for shear dominated flows share similar anisotropy characteristics. When convection is present, the anisotropy properties of the maximum TKE scales are not as easy to classify.

Vertical variance is limited by the surface, resulting in smaller peak spectral values which occur at shorter scales than for the horizontal variances. The interplay between the smaller scales for vertical motion and larger scales for horizontal motion and scalars such as temperature result in modified scales for the covariances. The scales of maximum heat flux and momentum flux are typically larger than the isotropic scales and smaller than or equal to the maximum TKE scale.

Sonic anemometer data from the CASES99 main tower are used to examine the relationship between stability and elevation above the surface and the various peak scales and anisotropy characteristics.

### 2. Data and analysis

Data are from the CASES99 field campaign which took place near Leon, Kansas, October 1999. The data are from the Campbell Scientific CSAT3 sonic anemometers at 5m and 50m on the main tower (Poulos et al, 2002). Data were recorded 20 times per second.

Multiresolution spectral analysis is used to determine the amount of the variance or covariance due to motion at different scales (Vickers and Mahrt 2003). Since this is time series data, for each hour ( $2^{16}$  data points or 54.6 min of data) each of the six variances and covariances of the

Reynolds stress tensor are broken down into the amount of the variance and covariance due to motion at different time scales and then converted into a spatial scale by multiplying by the mean wind speed for that hour as measured by that sonic. For the smaller scales, this can be interpreted as an eddy scale, but for the larger scales, the conditions for Taylor's hypothesis do not hold, and therefore the larger scales do not correspond to a physical eddy dimension. Although this analysis uses an oversampling method at scales in addition to the fundamental Haar scales, the area under the spectral curve is fairly closely related to the total flux (Howell and Mahrt 1997).

Once each variance and covariance is determined for each scale, a Reynolds stress tensor can be formed for each scale. The eigenvalues of each Reynolds stress tensor are used to evaluate the degree and nature of the anisotropy of the turbulence at that scale using the method of Banerjee, *et al.* (2007). Anisotropy has two degrees of freedom and therefore requires a minimum of two parameters to fully describe it: the degree of anisotropy as well as the axisymmetry of the variances (Choi and Lumley 2001). Although the method of Banerjee, *et al.* (2007) produces three parameters, only two are independent, so the anisotropy characteristics can be plotted on a plane using a barycentric plotting method.

For each scale, the diagonalized Reynolds stress tensor, non-dimensionalized by the trace, is decomposed into one dimensional, two dimensional and three dimensional basis tensors, with coefficients  $C_1$ ,  $C_2$ , and  $C_3$ . The vertices of the triangular barycentric plots (Figure 1) represent motion that is either three dimensional (fully isotropic) at  $C_3$ , two dimensional (one eigenvalue vanishes) at  $C_2$ , or one dimensional (two eigenvalues vanish) at  $C_1$ . The line from  $C_3$  to  $C_2$  represents pancake-like axisymmetry (two large identical eigenvalues, one small) and the line between  $C_3$  and  $C_1$  represents cigar-like axisymmetry (two small identical eigenvalues, one large). Purely isotropic turbulence will plot at the top vertex with  $C_3 = 1$  and  $C_1 = C_2 = 0$ . If the smallest eigenvalue vanishes then  $C_3 = 0$ ,

---

\* Corresponding author address: Cheryl Klipp, US Army Research Lab, attn RDRL-CIE-D, 2800 Powder Mill Rd., Adelphi, MD 20783. [cheryl.l.klipp.civ@mail.mil](mailto:cheryl.l.klipp.civ@mail.mil)

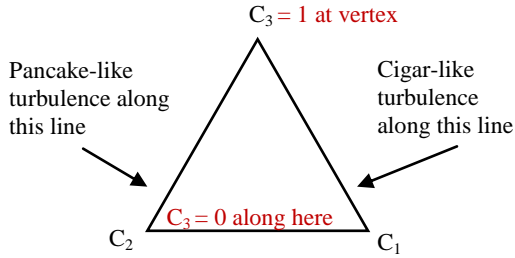


Figure 1: Diagram of the barycentric plot for turbulence parameters. See text for description.

the turbulence is two dimensional, and plots along the bottom line. Since this barycentric plot is linear in the eigenvalues (Banerjee *et al.* 2007), which are the fundamental variances for the flow, it is more practical to use than the more elegant Lumley turbulence triangle (Choi and Lumley, 2001).

Note that the variances and the eddies do not necessarily share the same axisymmetry (Choi and Lumley 2001, Simonsen and Krogstad 2005). Although it is possible to draw an inverse relationship between eddy axisymmetry and variance axisymmetry when anisotropy is produced in a wind tunnel, it is not clear if such a relationship exists in the atmosphere.

### 3. Results

Figure 2 is the multiresolution spectra of the six components of the Reynolds stress tensor for two levels and two different stability conditions. The night and day of 29 Oct, 1999 were chosen for the relatively stationary wind speed and direction. The winds are from the south, so little if any influence is expected from the tower. At the 5m level at 0200-0254 CST the local value for  $z/L$  is 0.031 and at 1100-1154 CST  $z/L = -0.015$ . For the same times at the 50m level, the local  $z/L = 0.26$  for 0200-0254 and  $z/L = -0.13$  for 1100-1154.

The variances  $u'u'$ ,  $v'v'$ , and  $w'w'$  have peak values at different scales, with  $w'w'$  (red) peaking at small scales, especially near the surface. For convective conditions, the  $v'v'$  spectral values (green) have more energy in larger scales compared to the stable and neutral conditions, with peak values occurring at scales larger than the  $u'u'$  peak scales (blue), which are similar in scale for all the stability conditions, depending heavily on elevation. At the smallest scales the variances are nearly equal to each other in value and the covariances are negligible. These scales are nearly isotropic.

The scales with the most energy are the scales responsible for the most transport. Since different variances have different peak scales, the peak scales of the covariances usually lies between the peak scales for the variances of the individual components. Take  $u'w'$  as an example. On the spectra in Figure 2, the peak scale for  $u'u'$  is larger than the peak scale for  $w'w'$  and the scale with the most negative value for  $u'w'$  (or largest  $|u'w'|$ ) lies between the two. Since the turbulent kinetic energy (TKE) is the sum of the three variances, TKE usually also peaks at an intermediate scale.

The barycentric plots in Figure 3 show the anisotropy of the spectra shown in Figure 2. The smallest scales are nearest the  $C_3$  point, but not right on it, especially at the lower elevation. At 50m above the surface, more scales are closer to isotropic than at 5m where the transition across the  $C_3 = 0.5$  line occurs at relatively small scales of motion. It is not known at this time if the turbulence is not exactly isotropic at the smallest scales or if it only appears that way due to instrument limitations. The scales of maximum TKE,  $u'w'$ ,  $v'w'$ , and  $w'T'$  are indicated. Note that only one of these scales has a  $C_3$  value greater than 0.5. Therefore the scales of motion responsible for the bulk of the flux values are not very isotropic.

Figure 4 plots the anisotropy of the peak TKE scales for every hour of relatively stationary data during the field campaign. The color indicates stability with neutral (or shear dominated) defined as  $-0.05 < z/L < 0.05$  for the 5m elevation and  $-0.1 < z/L < 0.1$  for the 50m elevation. For all of the 5m data and most of the 50m data, the peak TKE scales are very anisotropic. At 5m, most of the neutral and some of the stable data cluster near the  $C_2 = 0.5$  line. This area is also near the plane strain line and may be a common characteristic of shear dominated flows with two dimensional geometry. The behavior of the convective cases is different. Based on the spectra in Figure 2, these large scales are dominated by nearly equal contributions from the streamwise and cross-stream components with very little influence from vertical motion. The 50m data only slightly follows this clustering. It is possible that an assumption of two dimensional geometry is not a good approximation this far from the surface except for a few stable periods. The inappropriateness of assuming two dimensional geometry at the 50m elevation is also supported by the significant values of  $u'v'$  compared to the magnitude of the other covariances.

Figure 5 is the same as Figure 4 but for the scales with largest  $|u'w'|$ . Since the scales with the most momentum flux are in general slightly smaller than the scales with maximum TKE, the data are somewhat similar but shifted slightly upward closer to the  $C_3$  vertex. The locations of the convective data are shifted the most. Again, even at 50m almost all the peak momentum flux scales are far from isotropic with most  $C_3$  values less than 0.5. In Figure 6, the peak scales for the other component of  $u^*$ ,  $v'w'$ , have a different behavior. For most neutral and stable hours, the scale with maximum  $|v'w'|$  is less than the scale with maximum  $|u'w'|$ , and is therefore slightly more isotropic. For convective conditions the opposite is true.

Similar to  $u'w'$ , in Figure 7 the scales with maximum heat flux (largest  $|w'T'|$ ) are slightly smaller and slightly closer to isotropy than the scales of maximum TKE, but are still mostly quite anisotropic at 5m. At 50m, a significant number of hours have peak heat flux scales in the nearly isotropic quadrant with  $C_3 > 0.5$ . Information about the scales of maximum  $T'T'$  can be found in Klipp (2012).

#### 4. Conclusions

Most theories of turbulence assume at least local isotropy which is shown above to occur only at small scales, and not at the scales of maximum transport. The impact of this mismatch between theory and data needs to be assessed to see if better theories and models are needed.

#### References

- Banerjee, S., Krahl, R., Durst, F., and Zenger, Ch., 2007, "Presentation of anisotropy properties of turbulence, invariants versus eigenvalue approaches," *Journal of Turbulence*, vol. 8, DOI: 10.1080/14685240701506896.
- Choi, K.-S., and Lumley, J. L., 2001, "The return to isotropy of homogeneous turbulence," *Journal of Fluid Mechanics*, vol. 436, pp. 59-84.
- Howell, J. F. and L. Mahrt, 1997, "Multiresolution flux decomposition," *Boundary Layer Meteorology*, **83**, 117 – 137.
- Klipp, C., 2012, "Near-surface Turbulent Temperature Variances and Anisotropy at Multiple Scales of Motion," *Proc. SPIE*, vol. 8380, 8380-15.
- Poulos, G. S., Blumen, W., Fritts, D. C., Lundquist, J. K., Sun, J., Burns, S. P., Nappo, C., Banta, R., Newsom, R., Cuxart, J., Terradellas, E., Balsley, B., and Jensen, M., 2002, "CASES-99: A Comprehensive Investigation of the Stable Nocturnal Boundary Layer," *Bulletin of the American Meteorological Society*, vol. 83(4), pp. 555-581.
- Simonsen, A. J. and Krogstad, P.-A., 2005, "Turbulent stress invariant analysis: Clarification of existing terminology," *Physics of Fluids*, vol. 17, 088103, DOI:10.1063/1.2009008
- Vickers, D., and Mahrt, L., 2003, "The cospectral gap and turbulent flux calculations," *Journal of Atmospheric and Oceanic Technology*, vol. 20, pp. 660-672.

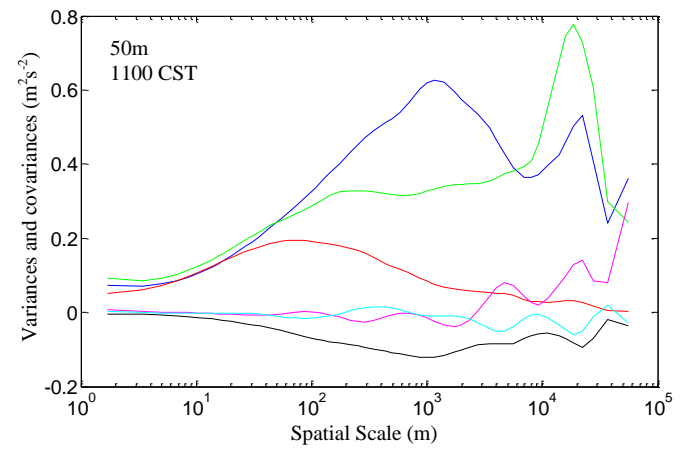
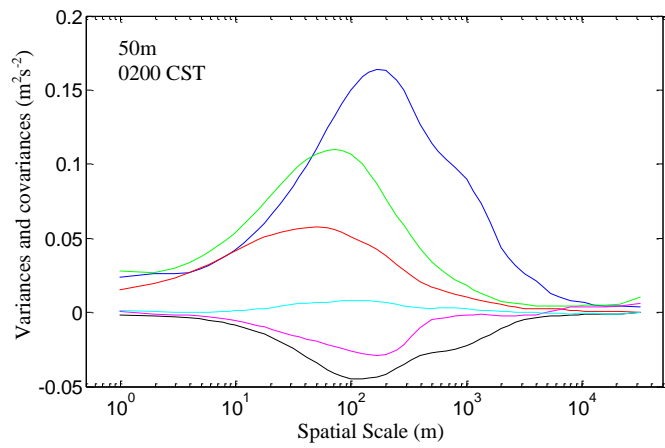
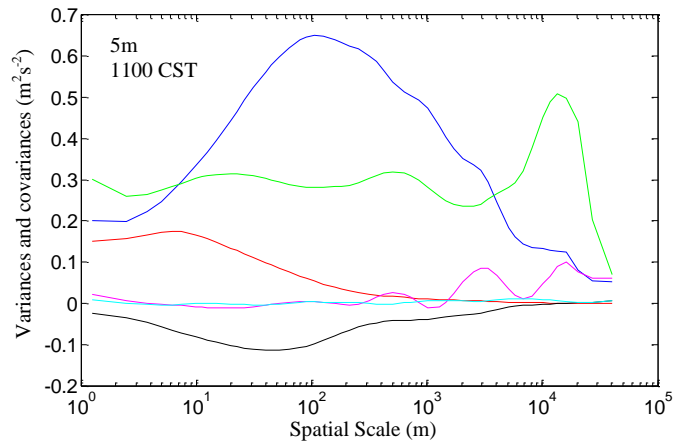
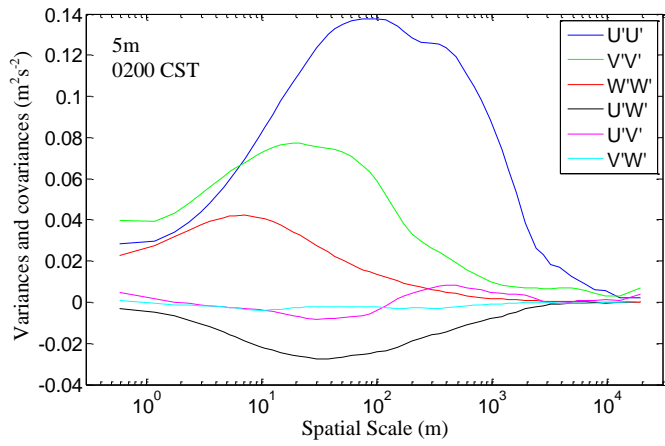


Figure 2: Multiresolution spectra of the six components of the Reynolds stress tensor for 29 Oct at 0200 and 1100 CST at both 5m and 50m agl.

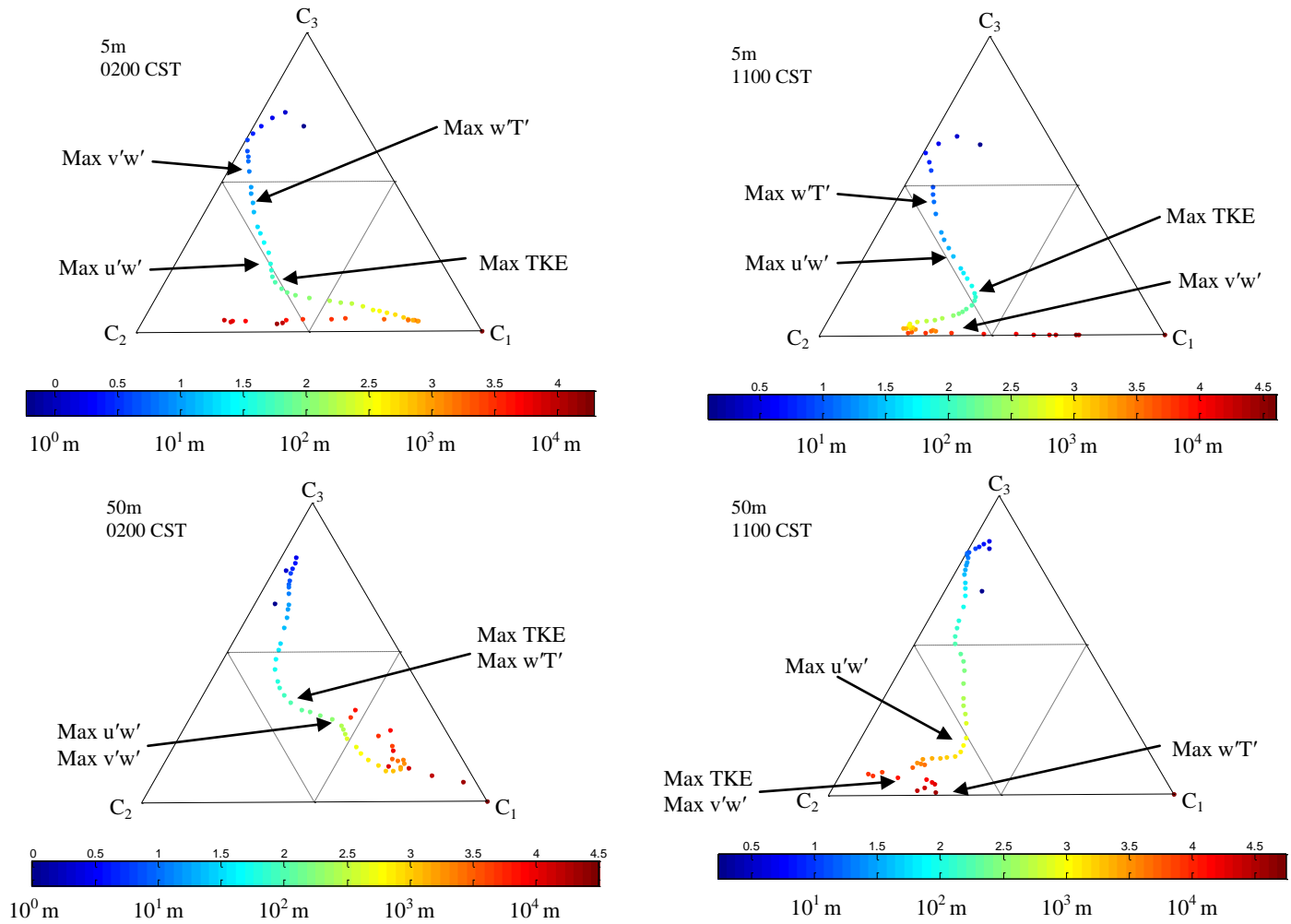


Figure 3: Barycentric plots of spectra in Figure 2. Scales of maximum TKE, heat flux and momentum flux components are indicated with arrows. Smaller scales are more isotropic and plot nearer the  $C_1$  vertex. The anisotropy of the larger scales varies, especially depending on stability.

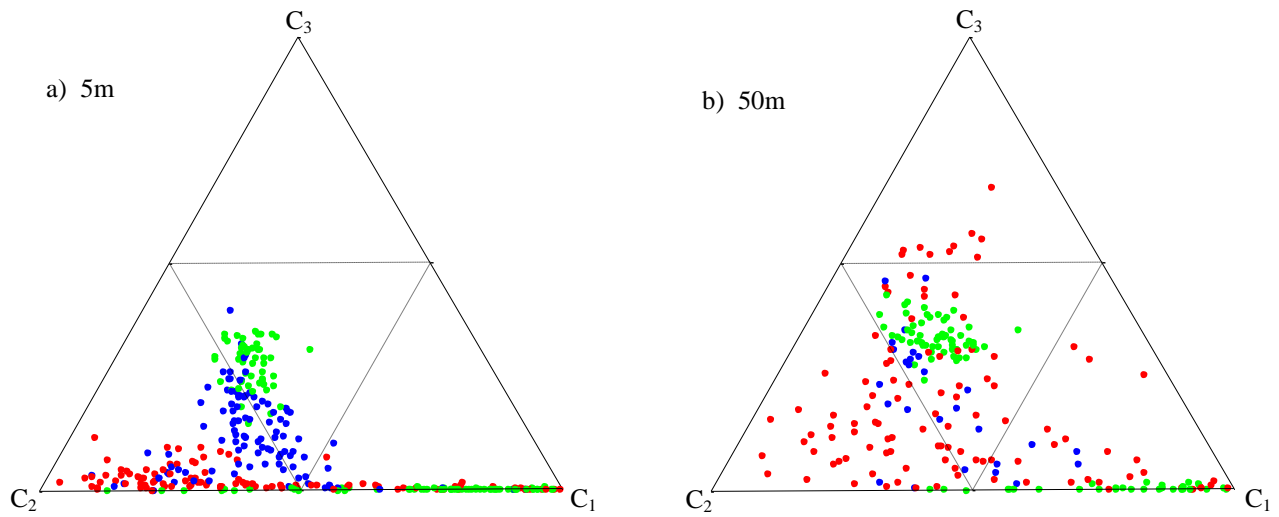


Figure 4 Barycentric plots of scale of maximum TKE for all available hours of CASES99. a) 5m Green are stable,  $z/L > 0.05$ , red are unstable/convective,  $z/L < -0.05$ , blue are remaining neutral points. b) 50m Green are stable,  $z/L > 0.1$ , red are unstable/convective,  $z/L < -0.1$ , blue are remaining neutral points.

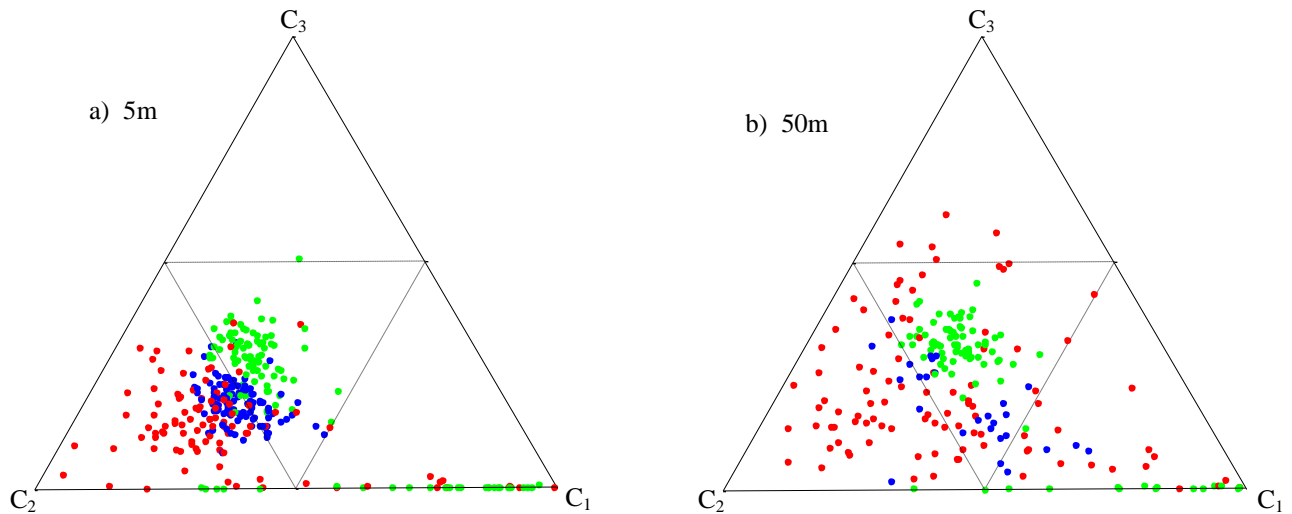


Figure 5: Barycentric plots of scale of maximum  $u'w'$  for all available hours of CASES99. a) 5m Green are stable,  $z/L > 0.05$ , red are unstable/convective,  $z/L < -0.05$ , blue are remaining neutral points. b) 50m Green are stable,  $z/L > 0.1$ , red are unstable/convective,  $z/L < -0.1$ , blue are remaining neutral points.

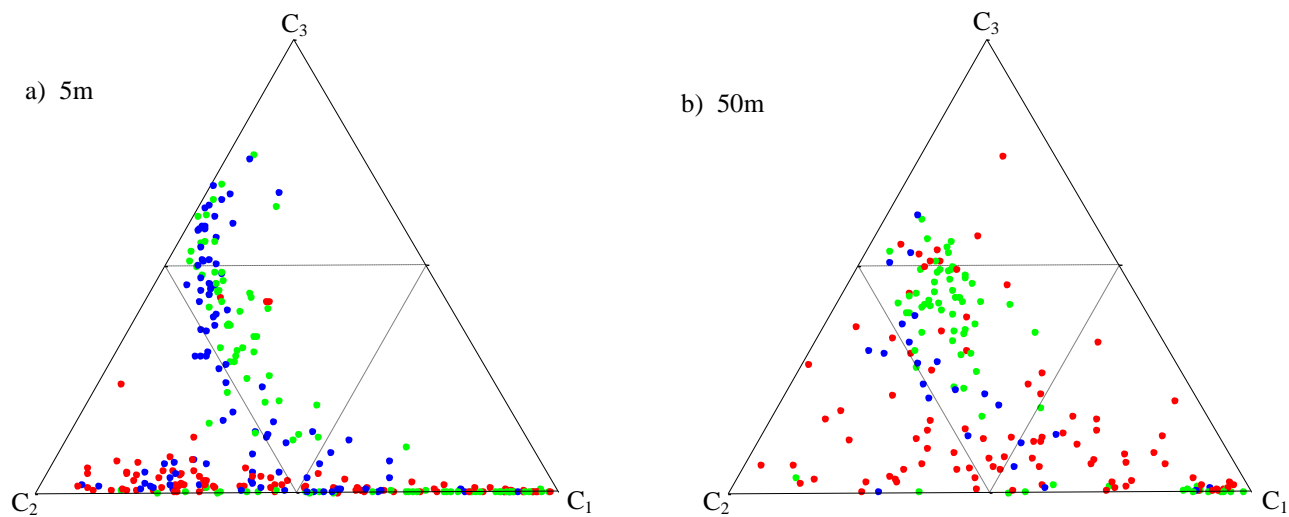


Figure 6: Barycentric plots of scale of maximum  $v'w'$  for all available hours of CASES99. a) 5m Green are stable,  $z/L > 0.05$ , red are unstable/convective,  $z/L < -0.05$ , blue are remaining neutral points. b) 50m Green are stable,  $z/L > 0.1$ , red are unstable/convective,  $z/L < -0.1$ , blue are remaining neutral points.

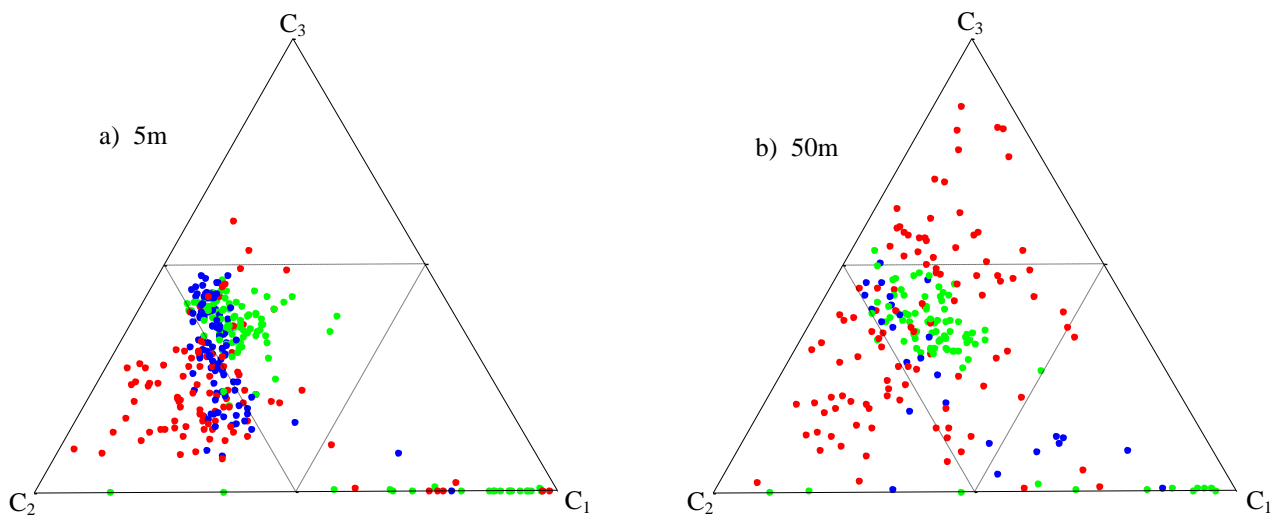


Figure 7: Barycentric plots of scale of maximum heat flux for all available hours of CASES99. a) 5m Green are stable,  $z/L > 0.05$ , red are unstable/convective,  $z/L < -0.05$ , blue are remaining neutral points. b) 50m Green are stable,  $z/L > 0.1$ , red are unstable/convective,  $z/L < -0.1$ , blue are remaining neutral points.